Structural Engineering and Mechanics, *Vol. 63, No. 3 (2017) 401-415*
DOI: https://doi.org/10.12989/sem.2017.63.3.401

Hygro-thermo-mechanical vibration and buckling of exponentially graded nanoplates resting on elastic foundations via nonlocal elasticity theory

Mohammed Sobhy*[1,2]

[1]*Department of Mathematics and Statistics, Faculty of Science, King Faisal University, P.O. Box 400, Hofuf, 31982, Saudi Arabia*
[2]*Department of Mathematics, Faculty of Science, Kafrelsheikh University, Kafrelsheikh 33516, Egypt*

(Received July 17, 2016, Revised May 16, 2017, Accepted May 17, 2017)

Abstract. In this article, hygro-thermo-mechanical vibration and buckling of exponentially graded (EG) nanoplates resting on two-parameter Pasternak foundations are studied using the four-unknown shear deformation plate theory. The material properties are presumed to change only in the thickness direction of the EG nanoplate according to two exponential laws distribution. The boundary conditions of the nanoplate may be simply supported, clamped, free or combination of them. To consider the small scale effect on forced frequencies and buckling, Eringen's differential form of nonlocal elasticity theory is employed. The accuracy of the present study is investigated considering the available solutions in literature. A detailed analysis is executed to study the influences of the plate aspect ratio, side-to-thickness ratio, temperature rise, moisture concentration and volume fraction distributions on the vibration and buckling of the nanoplates.

Keywords: nonlocal theory; exponentially graded nanoplate; hygro-thermo-mechanical loads; boundary conditions; vibration; buckling

1. Introduction

Since nanomaterials are essentially beneficial as electronic parts, so they can be accumulated to develop new strong composite materials and structures. Further, there is no a material to manufacture micro/nano-electro-mechanical (MEM/NEM) structural layers and achieve all material and economical requirements and integrate with the electronics on the same substrate. The multilayer or functionally graded layer can be used as a solution (Witvrouw and Mehta 2005). Functionally graded materials (FGMs) have been widely used in many applications such as electronics, optics, nuclear, biomedical, biology, chemistry, and mechanical engineering because of its superior mechanical, thermomechanical and electromechanical properties, comparing with the conventional laminated composites. Recently, FGMs have been employed in (MEM/NEM) systems (Witvrouw and Mehta 2005, Fu *et al*. 2004, Lee *et al*. 2006) thin films in the form of shape memory alloys (Fu *et al*. 2003, Craciunescu and Wuttig 2003), and atomic force microscopes (Rahaeifard *et al*. 2009). FGMs can be prescribed as heterogeneous composites that are composed from a mixture of two different materials with a desired continuous variation of properties as a function of position along certain dimension. These materials provide the specific advantages of both of the constituents.

Some studies have been devoted to demonstrate the different behaviors of the FGM nanostructures. Lü *et al*. (2009) have studied the surface effects on mechanical behavior of functionally graded ultra-thin films. Based on the differential quadrature method, Janghorban and Zare (2011) have investigated nonlocal natural frequency of FGM nanobeams. Eltaher *et al*. (2012) have investigated vibration response of FGM nanobeams using finite element formulation based on the Euler-Bernoulli beam theory. Natarajan *et al*. (2012) have demonstrated the natural frequency of size-dependent FG nanoplates using the finite element formulation and based on the nonlocal continuum theory of Eringen (1972, 1983, 2002). Şimşek and Yurtcu (2013) have studied the static bending and buckling of a functionally graded nanobeam based on the nonlocal Timoshenko and Euler-Bernoulli beam theories. Hashemi *et al*. (2013) have illustrated the free vibration response of circular and annular FG nanoplates using Eringen nonlocal elasticity theory. The nonlinear free vibration of FG nanobeams with simply supported-simply supported and simply supported-clamped boundary conditions, has been studied by Nazemnezhad and Hashemi (2014) using the nonlocal elasticity and Euler-Bernoulli beam theories. Based on the higher-order shear deformation beam theory and Eringen theory, the bending, buckling and vibration of FG nanobeams have been presented by Zemri *et al*. (2015). More reports on the behavior of FGM nanostructures may be also found in the open literature (see, e.g., Bouafia *et al*. 2017, Bounouara *et al*. 2016, Belkorissat *et al*. 2015).

For FGM nanostructures, the classical plate theory (CPT), in which the normal stress is neglected, will produce unsatisfying even incorrect results when material properties change suddenly due to the existing of complicated shear deformations (Lü *et al*. 2009). Therefore, many theories have been developed to take account the transverse deformations in FGM plates especially those with abrupt

∗Corresponding author, Ph.D.
E-mail: msobhy@kfu.edu.sa, msobhy2011@gmail.com

 ISSN: 1225-4568 (Print), 1598-6217 (Online)

variation of material properties. Reddy (2000) has employed the third-order shear deformation theory to study the static behavior of functionally graded plates. Based on the first-order and third-order shear deformation theories, Cheng and Batra (2000) have studied the bending of a FG plate with simply supported edges. Qian *et al*. (2003) have investigated the free and forced vibrations and bending of FG plate using a higher-order shear and normal deformable plate theory. Roque *et al*. (2007) have used the higher-order shear deformable plate theory to investigate the free vibration of FG plates with different combinations of boundary conditions. On the basis of the sinusoidal shear deformation plate theory, Zenkour and Sobhy (2010, 2011, 2012, 2013) and Sobhy (2013) have investigated the thermal buckling, bending, vibration and mechanical buckling of FGM plates and sandwich plates. Aydogdu and Taskin (2007) have illustrated the natural frequencies and mode shapes of a FGM simply supported beam using exponential shear deformation theory. Neves *et al*. (2011, 2012) have presented an original hyperbolic sine shear deformation theory for the bending and free vibration analysis of FG plates. Akavci (2014) has studied the thermal buckling of FGM plates using a hyperbolic shear deformation theory. Based on the isogeometric analysis, the bending, free vibration and buckling of the laminated composite and sandwich plates have been investigated by Thai *et al*. (2014 and 2015) using new shear deformation plate theories. The two-variable plate theory is first developed by Shimpi (2002) for isotropic (Shimpi 2002, Sobhy 2014) or orthotropic (Shimpi 2006, Narendar and Gopalakrishnan 2012) homogeneous plates. This theory is extended to contain four unknown functions to fit the FGM plates. The four-unknown shear deformation plate theory has been employed by Thai and Choi (2011) and Merdaci *et al*. (2011) to illustrate the behavior of FGM plates. This theory doesn't need a correction factor and it similar to CPT in some features as governing equation and boundary conditions.

Structures are often exposed to heat and moisture during manufacturing or use. The change of temperature and moisture leads to a reverse impact on the stiffness and strength of the composite materials. The effects of thermal or hygrothermal conditions on the FGM structures have been investigated in many papers (see, e.g., Beldjelili *et al*. 2016, Bouderba *et al*. 2016, Sobhy 2015a,c, 2016a).

There are no papers, up to now, have dealt with the hygrothermal effects on the exponentially graded nanoplates with various boundary conditions. Therefore, this paper aims to study the effect of moisture concentration, thermal gradient and in-plane external load on the vibration of EGM nanoplates resting on elastic foundations. Further, the mechanical buckling of EGM nanoplates is presented under the effect of the hygrothermal conditions. A new exponentially mixture law for the constituents of the nanoplate is presented. The four-unknown shear deformation theory (FPT) is employed to deduce the governing equations of motion. To investigate the nonlocality on forced vibration and buckling, Eringen's nonlocal theory is used. The material properties are presumed to be varied through the thickness utilizing two

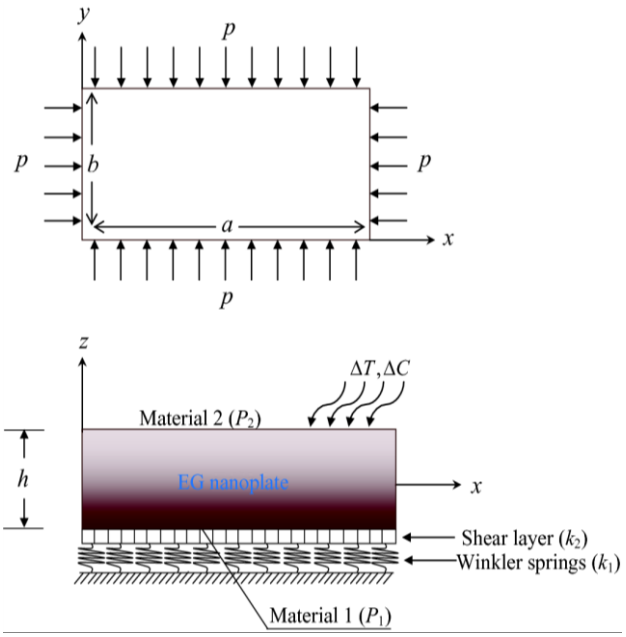

Fig. 1 EG nanoplate resting on elastic foundations and subjected to hygro-thermo-mechanical loads

exponential laws distribution. The analytical method is applied to solve the equations of motion for the plates with different combinations of free, clamped and simply supported boundary conditions at their edges. The displacement components are assumed by the author (see, Sobhy (2013, 2014a,b)) as trigonometric functions which satisfy the boundary conditions. To validate the present formulations, the given results are compared with those available in the literature. In addition, the influences played by nonlocal parameter, temperature rise and moisture concentration on the natural frequencies and buckling are all investigated.

2. Problem formulation

2.1 Plate construction

Fig. 1 shows a EG nanoplate of length a, width b and thickness h. The EG nanoplate is subjected to moisture exposure and elevated temperature and a compressive edge load in the x and y-directions. The $x_1 = x$, $x_2 = y$ and $x_3 = z$ coordinates are chosen along the length, width, and the thickness of EG nanoplates, respectively. The EG nanoplate is composed of two different materials at the top ($x_3 = h/2$) and the bottom ($x_3 = -h/2$) surfaces (as shown in Fig. 1). The effective material properties $[P(x_3)]$ of the EG nanoplate (i.e., Young's modulus $E(x_3)$, Poisson's ratio $\nu(x_3)$, mass density $\rho(x_3)$, thermal expansion coefficient $\gamma(x_3)$ and moisture expansion coefficient $\eta(x_3)$) vary continuously in the thickness direction (in x_3 direction). The effective material properties at any point may be determined according to two exponential laws as:

EGM1:

$$P(z) = P_1 e^{\alpha\left(\frac{x_3}{h}+\frac{1}{2}\right)} \quad (1)$$

where P_1 is the material properties of the bottom surface; hence $P_2 = P_1 e^{\alpha}$ stand for the top surface properties and α is a parameter (inhomogeneity parameter) that governs the material variation profile through the plate thickness and takes values greater than zero. In the case of $\alpha = 0$, the plate is fully homogeneous with material properties P_1.

EGM2:

$$P(z) = P_1\ e^{\bar{\beta}\left(\frac{x_3}{h}+\frac{1}{2}\right)^{\kappa}}, \qquad \bar{\beta} = \ln\left(\frac{P_2}{P_1}\right), \tag{2}$$

where κ is the non-negative parameter (inhomogeneity parameter) which dictates the material variation profile through the thickness of the plate. It is noted that $P(z) = P_2$ when $\kappa = 0$, and $P(z) = P_1$ when $\kappa \cong \infty$. Further, Eq. (2) indicates that the bottom surface of the plate ($x_3 = -h/2$) has the properties of material 1 (P_1) whereas the top surface ($x_3 = +h/2$) of the plate has the properties of material 2 (P_2).

2.2 Displacement field

Unlike the traditional higher-order shear deformation theories (Reddy 2000, Cheng and Batra 2000, Qian *et al.* 2003, Roque *et al*. 2007, Zenkour and Sobhy 2010, Aydogdu and Taskin 2007, Neves *et al*. 2011, Akavci 2014), the proposed higher-order (third-order, sinusoidal, exponential and hyperbolic) shear deformation theories contains four unknowns and has strong similarities with CPT in many aspects such as equations of motion, boundary conditions, and stress resultant expressions. These theories are based on assumption that the in-plane and transverse displacements consist of bending and shear parts. The transverse normal stress σ_{33} is neglected in these theories. While, the shear stresses σ_{13} and σ_{23} are zero at the top and bottom surfaces of the plate.

The generalized displacement field, taking into account the shear deformation effect, is presented as

$$\left.\begin{aligned} u(x_1,x_2,x_3,t) &= u_0(x_1,x_2,t) - x_3 w^b_{,1} - \Psi(x_3) w^s_{,1}, \\ v(x_1,x_2,x_3,t) &= v_0(x_1,x_2,t) - x_3 w^b_{,2} - \Psi(x_3) w^s_{,2}, \\ w(x_1,x_2,x_3,t) &= w^b(x_1,x_2,t) + w^s(x_1,x_2,t), \end{aligned}\right\} \tag{3}$$

where u_0 and v_0 are the displacement components of the point (x_1, x_2) in the mid-plane along the x_1 and x_2 directions, respectively. The superscripts *b* and *s* refer to the bending and shear components of the transverse displacement, respectively; $(\ )_{,i} = \partial(\ )/\partial x_i$. The shape function $\Psi(x_3) = x_3 - f(x_3)$, in which $f(x_3)$ is a function of x_3 and given as

- For third-order shear deformation theory (TPT) (Reddy 2000): $f = x_3\left[1 - \frac{4}{3}\left(\frac{x_3}{h}\right)^2\right]$.
- For sinusoidal shear deformation theory (SPT) (Touratier 1991): $f = \frac{h}{\pi}\sin\left(\frac{\pi x_3}{h}\right)$.
- For exponential shear deformation theory (EPT) (Karama *et al.* 2003): $f = x_3\ \mathrm{e}^{-2\left(\frac{x_3}{h}\right)^2}$.
- For hyperbolic shear deformation theory (HPT) (Soldatos 1992): $f = h\sinh\left(\frac{x_3}{h}\right) - x_3\cosh\left(\frac{1}{2}\right)$.

The strain components ε_{ij} compatible with the displacement field in Eq. (3) are

$$\begin{Bmatrix}\varepsilon_{11}\\ \varepsilon_{22}\\ \varepsilon_{12}\end{Bmatrix} = \begin{Bmatrix}\varepsilon^0_{11}\\ \varepsilon^0_{22}\\ \varepsilon^0_{12}\end{Bmatrix} + x_3\begin{Bmatrix}\eta^b_{11}\\ \eta^b_{22}\\ \eta^b_{12}\end{Bmatrix} + \Psi(x_3)\begin{Bmatrix}\eta^s_{11}\\ \eta^s_{22}\\ \eta^s_{12}\end{Bmatrix},\ \varepsilon_{33} = 0,$$
$$\begin{Bmatrix}\varepsilon_{13}\\ \varepsilon_{23}\end{Bmatrix} = f'(x_3)\begin{Bmatrix}\eta^s_{13}\\ \eta^s_{23}\end{Bmatrix}, \tag{4}$$

where

$$\begin{aligned} &\varepsilon^0_{11} = u_{0,1}, \quad \varepsilon^0_{22} = v_{0,2}, \quad \varepsilon^0_{12} = v_{0,1} + u_{0,2} \\ &\eta^b_{11} = -w^b_{,11}, \quad \eta^b_{22} = -w^b_{,22}, \quad \eta^b_{12} = -2w^b_{,12}, \\ &\eta^s_{11} = -w^s_{,11}, \quad \eta^s_{22} = -w^s_{,22}, \quad \eta^s_{12} = -2w^s_{,12}, \end{aligned} \tag{5}$$
$$\eta^s_{13} = w^s_{,1}, \quad \eta^s_{23} = w^s_{,2}.$$

The linear constitutive relations of an EG nanoplate can be written as

$$\begin{aligned} \sigma_{11} &= \frac{E(x_3)}{[1-\nu(x_3)^2]}\left[\varepsilon_{11} + \nu(x_3)\varepsilon_{22}\right] \\ &\quad - \frac{E(x_3)}{1-\nu(x_3)}[\gamma(x_3)\Delta T + \eta(x_3)\Delta C], \\ \sigma_{22} &= \frac{E(x_3)}{[1-\nu(x_3)^2]}\left[\varepsilon_{22} + \nu(x_3)\varepsilon_{11}\right] \\ &\quad - \frac{E(x_3)}{1-\nu(x_3)}[\gamma(x_3)\Delta T + \eta(x_3)\Delta C], \\ \sigma_{12} &= \frac{E(x_3)}{2[1+\nu(x_3)]}\,\varepsilon_{12}, \quad \sigma_{13} = \frac{E(x_3)}{2[1+\nu(x_3)]}\,\varepsilon_{13}, \\ \sigma_{23} &= \frac{E(x_3)}{2[1+\nu(x_3)]}\,\varepsilon_{23}, \end{aligned} \tag{6}$$

where ΔT and ΔC are the temperature rise and moisture concentration, respectively, which are varied uniformly through the thickness. We introduce the following definitions of stress resultants

$$\begin{aligned} \{N_{kl}, M^b_{kl}, M^s_{kl}\} &= \int_{-\frac{h}{2}}^{\frac{h}{2}}\{1, x_3, \Psi(x_3)\}\sigma_{kl}\,\mathrm{d}x_3, \\ Q_{k3} &= \int_{-h/2}^{h/2} f'(x_3)\,\sigma_{k3}\,\mathrm{d}x_3, \qquad k,l = 1,2. \end{aligned} \tag{7}$$

2.3 Nonlocal elasticity theory

The nonlocal elasticity theory is first developed by Eringen (1972, 1983, 2002). Further, he was the first of the presented a differential form of the nonlocal constitutive equation. Contrary to the classical (local) elasticity theory, the stress at a point is a function of strains at all points in the continuum. In this way, the nonlocal theory contains information about long range forces between atoms, and the internal length scale is introduced into the constitutive equations simply as material parameter to obtain the small scale effect. Eringen's nonlocal constitutive equation (Eringen 1972, 1983, 2002) is presented as (see also, (Sobhy 2015a,b,c, 2016a))

$$\mathcal{L}\,\boldsymbol{\tau}_{kl} = \sigma_{kl}, \ \ \mathcal{L} = 1 - \xi\nabla^2, \ \ \xi = (e_0\ell)^2, \qquad k,l = 1,2,3, \tag{8}$$

where $\boldsymbol{\tau}_{kl}$ are the nonlocal stresses, ∇^2 is the Laplacian operator, ℓ is an internal characteristic length and e_0 is a constant. Also, the nonlocal stress resultants $\left(\mathbf{N}_{kl}, \mathbf{M}^b_{kl}, \mathbf{M}^s_{kl}, \mathbf{Q}_{k3}\right)$ are related to the classical stress resultants $(N_{kl}, M^b_{kl}, M^s_{kl}, Q_{k3})$ according to the equations

$$\begin{gathered}\mathcal{L}\,\mathbf{N}_{kl} = N_{kl}, \quad \mathcal{L}\,\mathbf{M}^b_{kl} = M^b_{kl}, \quad \mathcal{L}\,\mathbf{M}^s_{kl} = M^s_{kl}, \\ \mathcal{L}\,\mathbf{Q}_{k3} = Q_{k3}.\end{gathered} \tag{9}$$

3. Equations of motion

It should be noted that the principal of virtual work is independent of constitutive relations. So, this principal can be applied to derive the motion equations of the FGM nanoplates as

$$\begin{gathered}0 = \int_A \{\Pi_k + \mathbf{N}_{kl}\delta\varepsilon^0_{kl} + \mathbf{M}^b_{kl}\delta\eta^b_{kl} + \mathbf{M}^s_{kl}\delta\eta^s_{kl} \\ +\mathbf{Q}_{k3}\delta\eta^s_{k3} + \left[R_f(w^b + w^s) - F_{kl}\left(w^b_{,kl} + w^s_{,kl}\right)\right] \\ \delta(w^b + w^s)\}dA, k, l = 1,2,\end{gathered} \tag{10}$$

where

$$\begin{gathered}\Pi_k = \left(J_{11}\ddot{u}_0 - J_{12}\ddot{w}^b_{,1} - J_{13}\ddot{w}^s_{,1}\right)\delta u_0 \\ -\left(J_{12}\ddot{u}_0 - J_{22}\ddot{w}^b_{,1} - J_{23}\ddot{w}^s_{,1}\right)\delta w^b_{,1} \\ -\left(J_{13}\ddot{u}_0 - J_{23}\ddot{w}^b_{,1} - J_{33}\ddot{w}^s_{,1}\right)\delta w^s_{,1} \\ +\left(J_{11}\ddot{v}_0 - J_{12}\ddot{w}^b_{,2} - J_{13}\ddot{w}^s_{,2}\right)\delta v_0 \\ -\left(J_{12}\ddot{v}_0 - J_{22}\ddot{w}^b_{,2} - J_{23}\ddot{w}^s_{,2}\right)\delta w^b_{,2} \\ -\left(J_{13}\ddot{v}_0 - J_{23}\ddot{w}^b_{,2} - J_{33}\ddot{w}^s_{,2}\right)\delta w^s_{,2} \\ +J_{11}(\ddot{w}^b + \ddot{w}^s)\delta(w^s + w^b),\end{gathered} \tag{11}$$

in which dot-superscript convention indicates the differentiation with respect to the time variable t and the inertias J_{kl}, $(k, l = 1,2,3)$ are defined as

$$\begin{gathered}\begin{bmatrix}J_{11} & J_{12} & J_{13}\\ J_{12} & J_{22} & J_{23}\\ J_{13} & J_{23} & J_{33}\end{bmatrix} = \int_{-\frac{h}{2}}^{\frac{h}{2}} \rho(x_3)[\bar{B}]\mathrm{d}x_3, \\ \bar{B} = \begin{bmatrix}1 & x_3 & \Psi\\ x_3 & x_3^2 & x_3\Psi\\ \Psi & x_3\Psi & \Psi^2\end{bmatrix}.\end{gathered} \tag{12}$$

The reaction force of the elastic foundations is given as $R_f(w^b + w^s)$, where the operator R_f is expressed as

$$R_f = k_1 - k_2\nabla^2, \tag{13}$$

in which k_1 and k_2 are the Winkler's and Pasternak's foundation stiffnesses. The in-plane edge loads F_{ij} are written as

$$\begin{gathered}F_{11} = p_{11} + N^T_{11} + N^C_{11}, \\ F_{22} = p_{22} + N^T_{22} + N^C_{22}, \quad F_{12} = 0,\end{gathered} \tag{14}$$

where (p_{11}, p_{22}), (N^T_{11}, N^T_{22}) and (N^C_{11}, N^C_{22}) are the normal in-plane forces due to the mechanical, temperature and moisture loads, respectively, which are given as

$$p_{11} = p_{22} = -p, \tag{15}$$

$$N^T_{11} = N^T_{22} = N_T = -\int_{-\frac{h}{2}}^{\frac{h}{2}} \frac{E(x_3)}{1-\nu(x_3)}\gamma(x_3)\Delta T\,\mathrm{d}x_3,$$

$$N^C_{11} = N^C_{22} = N_C = -\int_{-\frac{h}{2}}^{\frac{h}{2}} \frac{E(x_3)}{1-\nu(x_3)}\eta(x_3)\Delta C\,\mathrm{d}x_3.$$

Eqs. (14) and (15) lead to $F_{11} = F_{22} = F$. Substituting from Eq. (5) into Eq. (10) and integrating by parts, and collecting the coefficients of $\delta u_0, \delta v_0, \delta w^b$ and δw^s, the equations of motion are obtained as

$$\begin{gathered}\mathbf{N}_{11,1} + \mathbf{N}_{12,2} = J_{11}\ddot{u}_0 - J_{12}\ddot{w}^b_{,1} - J_{13}\ddot{w}^s_{,1}, \\ \mathbf{N}_{12,1} + \mathbf{N}_{22,2} = J_{11}\ddot{v}_0 - J_{12}\ddot{w}^b_{,2} - J_{13}\ddot{w}^s_{,2}, \\ \mathbf{M}^b_{11,11} + 2\mathbf{M}^b_{12,12} + \mathbf{M}^b_{22,22} + F\,\nabla^2(w^b + w^s) \\ -R_f(w^b + w^s) = J_{11}(\ddot{w}^b + \ddot{w}^s) + J_{12}\left(\ddot{u}_{0,1} + \ddot{v}_{0,2}\right) \\ -J_{22}\nabla^2\ddot{w}^b - J_{23}\nabla^2\ddot{w}^s, \\ \mathbf{M}^s_{11,11} + 2\mathbf{M}^s_{12,12} + \mathbf{M}^s_{22,22} + \mathbf{Q}_{13,1} + \mathbf{Q}_{23,2} \\ +F\,\nabla^2(w^b + w^s) - R_f(w^b + w^s) = J_{11}(\ddot{w}^b + \ddot{w}^s) \\ +J_{13}\left(\ddot{u}_{0,1} + \ddot{v}_{0,2}\right) - J_{23}\nabla^2\ddot{w}^b - J_{33}\nabla^2\ddot{w}^s.\end{gathered} \tag{16}$$

The boundary conditions of the present theory include specifying the following pairs

$$\begin{array}{lll} u_0 & \text{or} & \mathbf{N}_{11}n_1 + \mathbf{N}_{12}n_2 \\ v_0 & \text{or} & \mathbf{N}_{12}n_1 + \mathbf{N}_{22}n_2 \\ w^b & \text{or} & \widehat{\mathbf{M}}^b \\ w^b_{,1} & \text{or} & \mathbf{M}^b_{11}n_1 + 2\mathbf{M}^b_{12}n_2 \\ w^b_{,2} & \text{or} & \mathbf{M}^b_{22}n_2 \\ w^s & \text{or} & \widehat{\mathbf{M}}^s \\ w^s_{,1} & \text{or} & \mathbf{M}^s_{11}n_1 + 2\mathbf{M}^s_{12}n_2 \\ w^s_{,2} & \text{or} & \mathbf{M}^s_{22}n_2 \end{array} \tag{17}$$

where

$$\begin{gathered}\widehat{\mathbf{M}}^b = \left(\mathbf{M}^b_{11,1} + 2\mathbf{M}^b_{12,2} - J_{12}\ddot{u}_0 + J_{22}\ddot{w}^b_{,1} + J_{23}\ddot{w}^s_{,1}\right)n_1 \\ +\left(\mathbf{M}^b_{22,2} - J_{12}\ddot{v}_0 + J_{22}\ddot{w}^b_{,2} + J_{23}\ddot{w}^s_{,2}\right)n_2, \\ \widehat{\mathbf{M}}^s = (\mathbf{M}^s_{11,1} + 2\mathbf{M}^s_{12,2} + \mathbf{Q}_{13} - J_{13}\ddot{u}_0 + J_{23}\ddot{w}^b_{,1} \\ +J_{33}\ddot{w}^s_{,1})n_1 + (\mathbf{M}^s_{22,2} + \mathbf{Q}_{23} - J_{13}\ddot{v}_0 \\ +J_{23}\ddot{w}^b_{,2} + J_{33}\ddot{w}^s_{,2})\,n_2\end{gathered} \tag{18}$$

By substituting Eq. (6) into Eq. (7) with the help of Eq. (4), the stress resultants are obtained as

$$\begin{gathered}\mathcal{L}\begin{bmatrix}\mathbf{N}_{11}\\ \mathbf{M}^b_{11}\\ \mathbf{M}^s_{11}\end{bmatrix} = [\mathrm{A}]\begin{bmatrix}\varepsilon^0_{11}\\ \eta^b_{11}\\ \eta^s_{11}\end{bmatrix} + [\mathrm{B}]\begin{bmatrix}\varepsilon^0_{22}\\ \eta^b_{22}\\ \eta^s_{22}\end{bmatrix} + \begin{bmatrix}N_T\\ M^b_T\\ M^s_T\end{bmatrix} + \begin{bmatrix}N_C\\ M^b_C\\ M^s_C\end{bmatrix}, \\ \mathcal{L}\begin{bmatrix}\mathbf{N}_{22}\\ \mathbf{M}^b_{22}\\ \mathbf{M}^s_{22}\end{bmatrix} = [\mathrm{A}]\begin{bmatrix}\varepsilon^0_{22}\\ \eta^b_{22}\\ \eta^s_{22}\end{bmatrix} + [\mathrm{B}]\begin{bmatrix}\varepsilon^0_{11}\\ \eta^b_{11}\\ \eta^s_{11}\end{bmatrix} + \begin{bmatrix}N_T\\ M^b_T\\ M^s_T\end{bmatrix} + \begin{bmatrix}N_C\\ M^b_C\\ M^s_C\end{bmatrix}, \\ \mathcal{L}\begin{bmatrix}\mathbf{N}_{12}\\ \mathbf{M}^b_{12}\\ \mathbf{M}^s_{12}\end{bmatrix} = [C]\begin{bmatrix}\varepsilon^0_{12}\\ \eta^b_{12}\\ \eta^s_{12}\end{bmatrix}, \qquad \mathcal{L}\begin{bmatrix}\mathbf{Q}_{13}\\ \mathbf{Q}_{23}\end{bmatrix} = \mathrm{H}\begin{bmatrix}\eta^s_{13}\\ \eta^s_{23}\end{bmatrix},\end{gathered} \tag{19}$$

where

$$\begin{gathered}[\mathrm{A}] = \int_{-\frac{h}{2}}^{\frac{h}{2}} \frac{E(x_3)}{[1-\nu(x_3)^2]}[\bar{B}]\mathrm{d}x_3, \\ [\mathrm{B}] = \int_{-\frac{h}{2}}^{\frac{h}{2}} \frac{\nu(x_3)E(x_3)}{[1-\nu(x_3)^2]}[\bar{B}]\mathrm{d}x_3,\end{gathered} \tag{20}$$

$$[C] = \int_{-\frac{h}{2}}^{\frac{h}{2}} \frac{E(x_3)}{2[1+\nu(x_3)]}\,[\bar{B}]\mathrm{d}x_3,$$

$$\mathrm{H} = \int_{-\frac{h}{2}}^{\frac{h}{2}} \frac{E(x_3)}{2[1+\nu(x_3)]}\,[f'(x_3)]^2\mathrm{d}x_3,$$

$$\{M_T^b,\ M_T^s\} = -\int_{-\frac{h}{2}}^{\frac{h}{2}} \frac{E(x_3)}{1-\nu(x_3)}\gamma(x_3)\Delta T\,\{x_3,\ \Psi\}\,\mathrm{d}x_3,$$

$$\{M_C^b,\ M_C^s\} = -\int_{-\frac{h}{2}}^{\frac{h}{2}} \frac{E(x_3)}{1-\nu(x_3)}\eta(x_3)\Delta C\,\{x_3,\ \Psi\}\,\mathrm{d}x_3.$$

4. Exact solutions

In this section, an analytical method (that likes Navier solution procedure) is developed to determine the exact solutions of the motion Eq. (16) for hygro-thermo-mechanical vibration and buckling of FGM nanoplate under various boundary conditions. For this purpose, the displacement functions are expressed as product of undetermined coefficients and known trigonometric functions to satisfy the governing equations and the conditions at the edges of the plate. The following displacement fields are assumed to be of the form (Sobhy 2013)

$$\begin{aligned} u_0 &= \sum_m\sum_n U_{mn}\varphi_{m,1}(x_1)\psi_n(x_2)e^{I\omega_{mn}t},\\ v_0 &= \sum_m\sum_n V_{mn}\varphi_m(x_1)\psi_{n,2}(x_2)e^{I\omega_{mn}t},\\ \{w^b, w^s\} &= \sum_m\sum_n \{W_{mn}^b, W_{mn}^s\}\varphi_m(x_1)\psi_n(x_2)e^{I\omega_{mn}t}, \end{aligned} \tag{21}$$

where U_{mn}, V_{mn}, W_{mn}^b and W_{mn}^s are the unknown parameters and $\omega_{mn} = \omega$ denotes the eigenfrequency associated with (mth, nth) eigenmode. The functions $\varphi_m(x_1)$ and $\psi_n(x_2)$ are suggested here to satisfy the following boundary conditions (simply-supported (S), clamped (C) and free (F)) (Shen *et al.* 2003)

$$\mathrm{S}: \varphi_m(0) = \varphi_{m,11}(0) = \varphi_m(a) = \varphi_{m,11}(a) = 0,\quad \psi_n(0) = \psi_{n,22}(0) = \psi_n(b) = \psi_{n,22}(b) = 0, \tag{22}$$

$$\mathrm{C}: \varphi_m(0) = \varphi_{m,1}(0) = \varphi_m(a) = \varphi_{m,1}(a) = 0,\quad \psi_n(0) = \psi_{n,2}(0) = \psi_n(b) = \psi_{n,2}(b) = 0, \tag{23}$$

$$\mathrm{F}: \varphi_{m,11}(0) = \varphi_{m,111}(0) = \varphi_{m,11}(a) = \varphi_{m,111}(a) = 0,\quad \psi_{n,22}(0) = \psi_{n,222}(0) = \psi_{n,22}(b) = \psi_{n,222}(b) = 0. \tag{24}$$

The functions $\varphi_m(x_1)$ and $\psi_n(x_2)$ that satisfy the above boundary conditions are given as (Sobhy 2013, 2014a,b, Thai *et al.* 2014, Meziane *et al.* 2014)

$$\begin{aligned} &\mathrm{SS}:\ \varphi_m(x_1) = \sin(\theta x_1),\\ &\mathrm{CC}:\ \varphi_m(x_1) = \sin^2(\theta x_1),\\ &\mathrm{CS}:\ \varphi_m(x_1) = \sin(\theta x_1)\,[1-\cos(\theta x_1)],\\ &\mathrm{FF}:\ \varphi_m(x_1) = \cos^2(\theta x_1)\,[1+\sin^2(\theta x_1)], \theta = m\pi/a. \end{aligned} \tag{25}$$

Applying the operator $\mathcal{L}$ to the nonlocal governing Eq. (16) and substituting Eq. (19) into the resulting equations with the help of Eq. (21), one obtains the equations of motion in terms of the unknowns U_{mn}, V_{mn}, W_{mn}^b and W_{mn}^s as

$$([K] - \omega^2[L])\{\Upsilon\} = \{0\}, \tag{26}$$

where $\{\Upsilon\}$ stands for the vector

$$\{\Upsilon\}^T = \{U_{mn} \quad V_{mn} \quad W_{mn}^b \quad W_{mn}^s\}. \tag{27}$$

The elements of the matrices $[K]$ and $[L]$ are given as

$$\begin{aligned} K_{11} &= A_{11}e_3 + C_{11}e_2, \quad K_{12} = (B_{11}+C_{11})e_2,\\ K_{13} &= -A_{12}e_3 - (B_{12}+2C_{12})e_2,\\ K_{14} &= -A_{13}e_3 - (B_{13}+2C_{13})e_2,\\ K_{21} &= (B_{11}+C_{11})e_6, \quad K_{22} = A_{11}e_5 + C_{11}e_6,\\ K_{23} &= -A_{12}e_5 - (B_{12}+2C_{12})e_6,\\ K_{24} &= -A_{13}e_5 - (B_{13}+2C_{13})e_6,\\ K_{31} &= A_{12}e_{12} + (B_{12}+2C_{12})e_{11},\\ K_{32} &= A_{12}e_9 + (B_{12}+2C_{12})e_{11},\\ K_{33} &= -A_{22}(e_9+e_{12}) - 2(B_{22}+2C_{22})e_{11} + \hat{F},\\ K_{34} &= -A_{23}(e_9+e_{12}) - 2(B_{23}+2C_{23})e_{11} + \hat{F},\\ K_{41} &= A_{13}e_{12} + (B_{13}+2C_{13})e_{11},\\ K_{42} &= A_{13}e_9 + (B_{13}+2C_{13})e_{11},\\ K_{43} &= K_{34},\\ K_{44} &= -A_{33}(e_9+e_{12}) - 2(B_{33}+2C_{33})e_{11} + \mathrm{H}(e_8+e_{10}) + \hat{F}, \end{aligned} \tag{28}$$

$$\begin{aligned} L_{11} &= J_{11}[\xi(e_2+e_3) - e_1], \quad L_{12} = 0,\\ L_{13} &= -J_{12}[\xi(e_2+e_3) - e_1],\\ L_{14} &= -J_{13}[\xi(e_2+e_3) - e_1], \quad L_{21} = 0,\\ L_{22} &= J_{11}[\xi(e_5+e_6) - e_4],\\ L_{23} &= -J_{12}[\xi(e_5+e_6) - e_4],\\ L_{24} &= -J_{13}[\xi(e_5+e_6) - e_4],\\ L_{31} &= J_{12}[\xi(e_{11}+e_{12}) - e_{10}],\\ L_{32} &= J_{12}[\xi(e_9+e_{11}) - e_8],\\ L_{33} &= \xi[J_{11}(e_8+e_{10}) - J_{22}(e_9+2e_{11}+e_{12})] - J_{11}e_7 + J_{22}(e_8+e_{10}),\\ L_{34} &= \xi[J_{11}(e_8+e_{10}) - J_{23}(e_9+2e_{11}+e_{12})] - J_{11}e_7 + J_{23}(e_8+e_{10}),\\ L_{41} &= J_{13}[\xi(e_{11}+e_{12}) - e_{10}],\\ L_{42} &= J_{13}[\xi(e_9+e_{11}) - e_8], \quad L_{43} = L_{34},\\ L_{44} &= \xi[J_{11}(e_8+e_{10}) - J_{33}(e_9+2e_{11}+e_{12})] - J_{11}e_7 + J_{33}(e_8+e_{10}), \end{aligned} \tag{29}$$

in which

$$\begin{aligned} \hat{F} &= [\xi(e_8+e_{10}) - e_7]k_1\\ &-[\xi(e_9+2e_{11}+e_{12}) - e_8 - e_{10}](k_2 - p + N_T + N_C), \end{aligned} \tag{30}$$

$$\begin{aligned} &\{e_1, e_2, e_3\}\\ &= \int_{x_1=0}^{a}\int_{x_2=0}^{b} \begin{Bmatrix} \varphi_{m,1}\psi_n, \varphi_{m,1}\psi_{n,22},\\ \varphi_{m,111}\psi_n \end{Bmatrix} \varphi_{m,1}\psi_n\,\mathrm{d}x_2\mathrm{d}x_1,\\ &\{e_4, e_5, e_6\}\\ &= \int_{x_1=0}^{a}\int_{x_2=0}^{b} \begin{Bmatrix} \varphi_m\psi_{n,2}, \varphi_m\psi_{n,222},\\ \varphi_{m,11}\psi_{n,2} \end{Bmatrix} \varphi_m\psi_{n,2}\,\mathrm{d}x_2\mathrm{d}x_1,\\ &\{e_7, e_8, e_9\} = \int_{x_1=0}^{a}\int_{x_2=0}^{b} \begin{Bmatrix} \psi_n, \psi_{n,22},\\ \psi_{n,2222} \end{Bmatrix} \varphi_m^2\psi_n\,\mathrm{d}x_2\mathrm{d}x_1,\\ &\{e_{10}, e_{11}, e_{12}\} \end{aligned} \tag{31}$$

$$= \int_{x_1=0}^{a}\int_{x_2=0}^{b} \begin{Bmatrix} \varphi_{m,11}\psi_n, \varphi_{m,11}\psi_{n,22}, \\ \varphi_{m,1111}\psi_n \end{Bmatrix} \varphi_m\psi_n \, \mathrm{d}x_2\mathrm{d}x_1.$$

In order to obtain the non-trivial solution, the determinant $|[K]-\omega^2[L]|$ should be equal to zero. Solving this determinant gives the eigenfrequencies ω. Whereas for the buckling analysis, we put $\omega = 0$ and then solve the determinant $|K|$ with respect to the mechanical load p.

5. Numerical examples and discussions

Two types of EG nanoplates are demonstrated in this study which their properties are varied through-the-thickness according to Eqs. (1) and (2). The material 1 of EGM1 nanoplate is taken as stainless steel (SUS304) which possesses the following mechanical properties (Natarajan *et al.* 2012): $E_1 = 201.04$ GPa, $\rho_1 = 8166$ kg/m^3. The EGM2 nanoplate is assumed to be made of silicon nitride (Si_3N_4) (ceramic) and stainless steel (SUS304) (metal). The mechanical properties of Si_3N_4 are (Natarajan *et al.* 2012): $E_2 = 348.43$ GPa, $\rho_2 = 2370$ kg/m^3. The thermal expansion coefficients γ (Sobhy and Radwan 2017) and moisture expansion coefficients η (Sobhy 2016b) are given for the metal as $\gamma_1 = 17.3\times10^{-6}$ K^{-1} and $\eta_1 = 0.44$ (wt.% H_2O)$^{-1}$ and for the ceramic as $\gamma_2 = 3.3\times10^{-6}$ K^{-1} and $\eta_2 = 0.001$ (wt.% H_2O)$^{-1}$. Poisson's ratio is presumed as a constant value $\nu = 0.3$. The nonlocal parameter is taken as $0 \le \xi \le 4$ nm^2, as proposed by Wang and Wang (2007), to study the nonlocal effects on the vibration and buckling of EG nanoplates. The following values of the different parameters are used in the numerical examples, unless otherwise stated: $\frac{b}{h} = 15, \frac{a}{b} = 1$, $b = 10$ nm, $g_1 = g_2 = 10$, $\xi = 1$ nm^2, $\Delta T = 30$ K, $\Delta C = 0.02$ %, $\kappa = 1$, $\alpha = 1$, $m = n = 1$.

The obtained results are expressed in terms of the following dimensionless parameters:

$$\widehat{\Omega} = \omega h\sqrt{\frac{\rho}{G}}, \quad G = \frac{E_2}{2(1+\nu)}, \quad g_1 = \frac{K_1 a^4}{D}, \quad g_2 = \frac{K_2 a^2}{D}, \quad D = \frac{E_2 h^3}{12(1-\nu^2)},$$

$$\bar{\Omega} = \omega a^2\sqrt{\frac{\rho h}{D}}, \quad \Omega = \frac{\omega b^2}{\pi^2}\sqrt{\frac{\rho h}{D}} \quad \Gamma = \frac{pa^2}{D\pi^2}.$$

In this section, various numerical examples are presented and compared with those being in the literature to verify the accuracy of the present solution of the free vibration of local and nonlocal plate. Table 1 shows the comparison of nondimensional free vibration of homogeneous isotropic plate obtained by the present theories with that given by Srinivas *et al.* (1970) using 3D elasticity theory, Reddy (1984) using a higher- and first-order shear deformation theories (HDPT and FDPT) and Shimpi and Patel (2006) employing the two variable

Table 1 Comparison of fundamental natural frequency $\widehat{\Omega}$ of a simply supported homogeneous square plate $(a/h = 10, g_1 = g_2 = 0)$

m	n	Source				Present			
		Exact (Srinivas *et al.* 1970)	HDPT (Reddy 1984)	FDPT (Reddy 1984)	RPT (Shimpi and Patel 2006)	TPT	SPT	EPT	HPT
1	1	0.09315	0.0931	0.0930	0.0930	0.09303	0.09303	0.09304	0.09303
1	2	0.22260	0.2222	0.2219	0.2220	0.22195	0.22198	0.22204	0.22195
2	2	0.34207	0.3411	0.3406	0.3406	0.34063	0.34069	0.34084	0.34063
1	3	0.41714	0.4158	0.4149	0.4151	0.41507	0.41516	0.41538	0.41507
2	3	0.52391	0.5221	0.5206	0.5208	0.52081	0.52096	0.52131	0.52081
1	4	---	0.6545	0.6520	0.6525	0.65249	0.65273	0.65327	0.65248
3	3	0.68893	0.6862	0.6834	0.6840	0.68396	0.68423	0.68483	0.68395
2	4	0.75111	0.7481	0.7446	0.7454	0.74536	0.74569	0.74640	0.74534
3	4	---	0.8949	0.8896	0.8908	0.89083	0.89132	0.89234	0.89080
1	5	0.92678	0.9230	0.9174	0.9187	0.91869	0.91922	0.92031	0.91866
2	5	---	1.0053	0.9984	1.0001	1.00008	1.00073	1.00203	1.00005
4	4	1.0889	1.0847	1.0764	1.0785	1.07845	1.07923	1.08074	1.07842
3	5	---	1.1361	1.1268	1.1292	1.12917	1.13004	1.13170	1.12913

Table 2 Comparison of fundamental natural frequency $\bar{\Omega}$ of a simply supported homogeneous square plate

g_1	g_2	Source		Present			
		Lam *et al.* (2000)	Baferani *et al.* (2011)	TPT	SPT	EPT	HPT
0	0	19.74	19.7374	19.73921	19.73921	19.73921	19.73921
	10^2	48.62	48.6149	48.61643	48.61643	48.61643	48.61643
	10^3	141.92	141.8730	141.87616	141.87616	141.87616	141.87616
10^2	0	22.13	22.1261	22.12773	22.12773	22.12773	22.12773
	10^2	49.63	49.6327	49.63423	49.63423	49.63423	49.63423
	10^3	142.20	142.2250	142.22814	142.22814	142.22814	142.22814
10^3	0	37.28	37.2763	37.27783	37.27783	37.27783	37.27783
	10^2	58.00	57.9945	57.99618	57.99618	57.99618	57.99618
	10^3	145.43	145.3545	145.35764	145.35764	145.35764	145.35764

Table 3 Comparison of fundamental natural frequency $\widehat{\Omega}$ of a simply supported homogeneous square plate $(a/h = 10, g_1 = g_2 = 0)$

m	n	ξ	Source				Present			
			Exact (Srinivas *et al.* 1970)	HDPT (Aghababaei and Reddy 2009)	FDPT (Aghababaei and Reddy 2009)	CPT (Aghababaei and Reddy 2009)	TPT	SPT	EPT	HPT
1	1	0	0.09315	0.0935	0.0930	0.0963	0.0930	0.0930	0.0930	0.0930
		1	---	0.0854	0.0850	0.0880	0.0850	0.0850	0.0850	0.0850
		2	---	0.0791	0.0788	0.0816	0.0788	0.0788	0.0788	0.0787
		3	---	0.0741	0.0737	0.0763	0.0737	0.0737	0.0737	0.0737
		4	---	0.0699	0.0696	0.0720	0.0695	0.0695	0.0696	0.0695
		5	---	0.0663	0.0660	0.0683	0.0660	0.0660	0.0660	0.0660
2	2	0	0.34207	0.3458	0.3414	0.3853	0.3406	0.3407	0.3409	0.3406
		1	---	0.2585	0.2552	0.2880	0.2546	0.2547	0.2548	0.2546
		2	---	0.2153	0.2126	0.2399	0.2121	0.2121	0.2122	0.2121
		3	---	0.1884	0.186	0.2099	0.1856	0.1856	0.1857	0.1856
		4	---	0.1696	0.1674	0.1889	0.1670	0.1671	0.1672	0.1670
		5	---	0.1555	0.1535	0.1732	0.1531	0.1532	0.1532	0.1531
3	3	0	0.68893	0.7020	0.6889	0.8669	0.6840	0.6843	0.6848	0.6840
		1	---	0.4213	0.4134	0.5202	0.4105	0.4106	0.4110	0.4105
		2	---	0.3290	0.3228	0.4063	0.3205	0.3206	0.3209	0.3205
		3	---	0.2790	0.2738	0.3446	0.2719	0.2720	0.2722	0.2718
		4	---	0.2466	0.2420	0.3045	0.2402	0.2403	0.2405	0.2402
		5	---	0.2233	0.2191	0.2757	0.2176	0.2176	0.2179	0.2176

Table 4 Nondimensional frequency Ω of EGM2 square plate under various boundary conditions ($g_1 = g_2 = 100, p = 1$ GPa, $\Delta T = 100$ K)

$\frac{b}{h}$	Theory	Boundary conditions							
		SSSS	CSSS	CCSS	CCCS	CCCC	FFSS	FFCC	CSFF
					Ω_1				
5	TPT	2.62950	3.27820	3.46715	4.27120	4.26708	3.54288	4.34692	4.34218
	SPT	2.62950	3.27820	3.46716	4.27120	4.26710	3.54290	4.34698	4.34220
	EPT	2.62950	3.27820	3.46717	4.27123	4.26722	3.54291	4.34718	4.34226
	HPT	2.62950	3.27844	3.46800	4.27677	4.28226	3.54390	4.37203	4.35182
10	TPT	3.34872	3.94878	3.92391	4.43103	4.40441	4.03594	4.49613	4.51794
	SPT	3.34872	3.94880	3.92394	4.43107	4.40446	4.03599	4.49621	4.51801
	EPT	3.34875	3.94887	3.92404	4.43122	4.40466	4.03616	4.49647	4.51821
	HPT	3.34896	3.94966	3.92518	4.43337	4.40738	4.03811	4.50042	4.52132
15	TPT	3.20984	3.80271	3.78570	4.28876	4.26952	3.90645	4.36982	4.38312
	SPT	3.20984	3.80272	3.78573	4.28878	4.26956	3.90650	4.36986	4.38315
	EPT	3.20985	3.80277	3.78579	4.28888	4.26968	3.90658	4.37002	4.38328
	HPT	3.20986	3.80283	3.78586	4.28907	4.26992	3.90674	4.37040	4.38357
25	TPT	2.34227	2.82700	2.84730	3.25352	3.26618	2.98228	3.37802	3.35940
	SPT	2.34227	2.82700	2.84732	3.25352	3.26620	2.98230	3.37805	3.35942
	EPT	2.34228	2.82702	2.84738	3.25360	3.26628	2.98235	3.37812	3.35948
	HPT	2.34227	2.82700	2.84732	3.25352	3.26620	2.98230	3.37805	3.35942
					Ω_2				
5	TPT	11.2180	11.4545	11.5472	11.6904	11.7594	11.7256	11.8885	11.8145
	SPT	11.2153	11.4521	11.5452	11.6884	11.7576	11.7238	11.8868	11.8126
	EPT	11.2214	11.4572	11.5498	11.6924	11.7612	11.7276	11.8900	11.8161
	HPT	4.52501	5.49750	6.12365	6.39150	6.57415	6.95420	7.10025	7.05005
10	TPT	40.2995	39.3252	38.7444	38.2407	37.7569	37.9162	37.1183	37.6502
	SPT	40.2888	39.3151	38.7349	38.2315	37.7481	37.9077	37.1102	37.6416
	EPT	40.3191	39.3431	38.7620	38.2570	37.7727	37.9328	37.1335	37.6659
	HPT	8.91624	10.8045	12.0998	12.5518	12.9128	13.7711	13.9918	13.9088
15	TPT	88.6598	85.5590	83.8096	82.1236	80.6522	81.2238	78.6356	80.2725
	SPT	88.6354	85.5360	83.7876	82.1020	80.6314	81.2031	78.6158	80.2520
	EPT	88.7061	85.6026	83.8521	82.1643	80.6919	81.2644	78.6735	80.3118
	HPT	13.3562	16.1775	18.1227	18.7888	19.3275	20.6288	20.9482	20.8274
25	TPT	243.360	233.401	227.893	222.368	217.707	219.644	211.232	216.448
	SPT	243.292	233.337	227.830	222.307	217.648	219.585	211.176	216.389
	EPT	243.492	233.527	228.015	222.486	217.823	219.762	211.344	216.563
	HPT	22.2550	26.9442	30.1860	31.2870	32.1822	34.3605	34.8842	34.6855

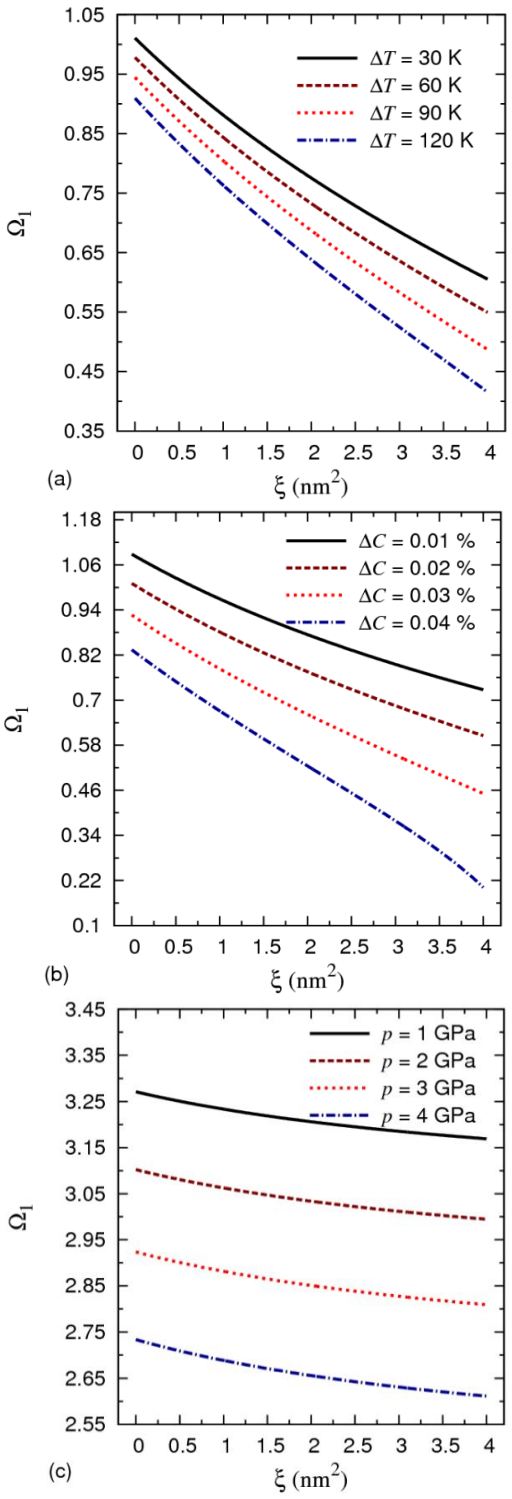

Fig. 2 First dimensionless frequency Ω_1 of the EGM2 square plate ($g_1 = g_2 = 100$) versus the nonlocal parameter ξ for various values of (a) temperature rise ΔT ($\Delta C = 0.02$ %, $p = 10$ GPa), (b) moisture concentration ΔC ($\Delta T = 30$ K, $p = 10$ GPa) and (c) in-plane mechanical load p ($\Delta T = 30$ K, $\Delta C = 0.02$ %)

refined plate theory (RPT). It can be seen that the present results of TPT, SPT and EPT are very agree with the published results for all values of mod numbers.

Table 2 exhibits the comparison of fundamental natural frequency of a simply supported homogeneous square plate without or resting on elastic foundations. The obtained results are compared with those presented by Lam *et al.* (2000) using Green's functions and Baferani *et al.* (2011) based on the third-order shear deformation plate theory. It can be seen that an excellent agreement is obtained for all values of elastic foundation parameters.

Another comparison study is carried out for free vibration of a simply supported homogeneous square nonlocal nanoplte. The nondimensional natural frequency $\widehat{\Omega}$ of a nanoplate obtained by the present shear deformation theories is compared with that obtained by Aghababaei and Reddy (2009) for various values of nonlocal parameter as shown in Table 3. Again, an excellent agreement is obtained for all values of nonlocal parameter.

The effects of the side-to-thickness ratio and boundary conditions on the first and second frequencies of EGM2 square nanoplate resting on elastic foundations are examined in Tables 4. The results are presented based on the TPT, SPT, EPT and HPT. It is to be noted that the change of boundary condition leads to a significant variation in the frequencies. A noticeable difference between the frequencies Ω_2 obtained by the HPT and those obtained by other theories is also shown in Table 4. This difference increases as the side-to-thickness ratio increases. It is also noticed that the first frequency increases and then decreases as the b/h increases while the second frequency directly increases with the increase of the ratio b/h.

The influences of the temperature rise ΔT, moisture concentration ΔC and in-plane load p on the variation of the first frequency Ω_1 of simply supported EGM2 nanoplates resting on two-parameter elastic foundations versus the nonlocal parameter ξ are shown in Fig. 2. On the basis of the SPT, the results in this figure and also in the following figures are drawn. It is seen that the temperature ΔT, moisture concentration ΔC and in-plane load p have the same effects on the vibration of nanoplates, with the increase of them the frequency Ω_1 decreases. Moreover, regardless of the external load effects, the frequency Ω_1 decreases monotonically as the nonlocal parameter ξ increases.

Figs. 3 and 4 display the variation of the first and second frequencies of simply supported EGM1 and EGM2 nanoplates versus the side-to-thickness ratio for different values of the nonlocal parameter ξ. It is noted from Fig. 3a that the first frequency Ω_1 of EGM1 nanoplate decreases to reach its minimum at $b/h = 11.3, 10.8, 10.4$ and 10.1 for $\xi = 0, 1, 2$ and 3, respectively. An abrupt change in the responses occurs at $b/h = 11.35, 10.85, 10.45$ and 10.15 for $\xi = 0, 1, 2$ and 3, respectively. The frequency Ω_1 varies linearly after these points. However, the first frequency Ω_1 of EGM2 nanoplate increases rapidly to reach its maximum and then decreases as the side-to-thickness ratio increases. Whereas, the second frequencies Ω_2 of EGM1 and EGM2 nanoplates have the same behavior with the variation of b/h, as shown in Figs. 3(b) and 4(b). Further, it is found that the difference between curves becomes important as the ratio b/h increases.

The effects of plate aspect ratio a/b on the first and second frequencies of simply supported EGM1 and EGM2

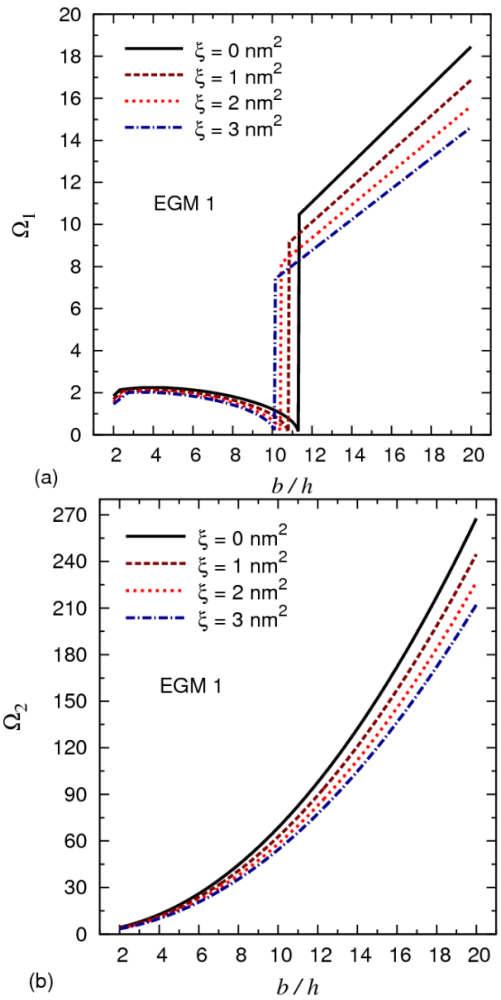

Fig. 3 (a) First dimensionless frequency Ω_1 and (b) second dimensionless frequency Ω_2 of the EGM1 square plate versus the side-to-thickness ratio b/h for various values the nonlocal parameter ξ $(p = 0)$

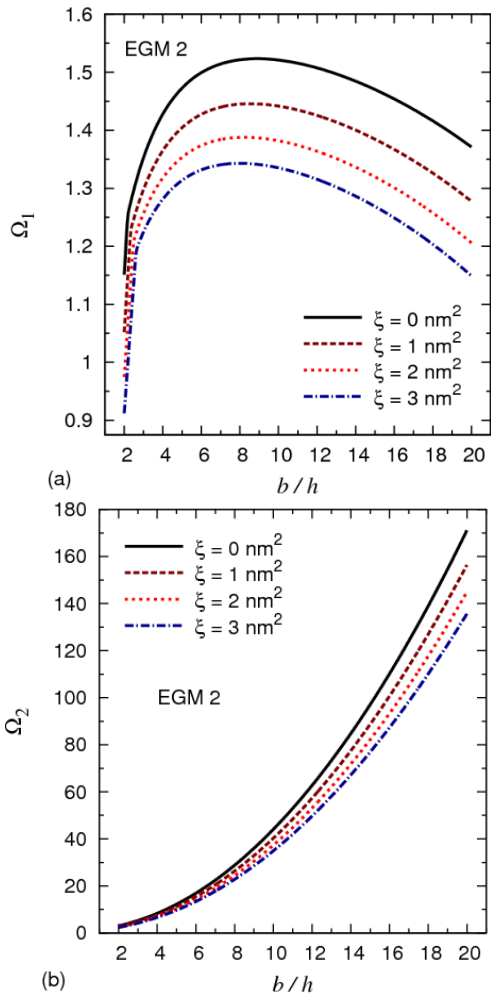

Fig. 4 (a) First dimensionless frequency Ω_1 and (b) second dimensionless frequency Ω_2 of the EGM2 square plate versus the side-to-thickness ratio b/h for various values the nonlocal parameter ξ $(p = 0)$

nanoplates are investigated in Figs. 5 and 6 for different values of the nonlocal parameter ξ. With the variation of a/b, the first frequency Ω_1 of EGM1 nanoplate has a singular sense (see, Fig. 5(a)), it decreases rapidly to get their lowest values then increases suddenly to get their highest values and then decreases gradually as the ratio a/b increases. Fig. 6(a) shows that, irrespective of the nonlocal parameter ξ, the first frequency Ω_1 of EGM2 nanoplate decreases smoothly as the ratio a/b varies. From Figs. 5(b) and 6(b), significant difference between the behavior of local and nonlocal frequencies is noted, indicating the small scale effect.

Fig. 7 reveals the effect of elastic foundation parameters on the first frequency Ω_1 of the simply supported EGM2 nanoplate for various values of ξ. It is clear that the frequency Ω_1 is strongly affected by the presence of the elastic foundations. Without elastic foundations, the frequency Ω_1 varies nonlinearly with the change in the side-to-thickness ratio b/h. While, with the presence of elastic foundations $(g_1 = g_2 = 10^4)$, the frequency Ω_1 varies linearly as the ratio b/h increases. However, for $g_1 = g_2 = 10^2$, the frequency Ω_1 is linearly dependent on b/h when $b/h < 5.8, 6.3, 6.95$ and 7.23 for $\xi = 0, 1, 2$ and 3. Then, it is weakly dependent on b/h after those values of b/h.

The effects of mode numbers m and n on free vibration ($\Delta T = \Delta C = p = 0$), mechanical vibration ($\Delta T = \Delta C = 0$, $p = 1$ GPa), thermal vibration ($\Delta T = 60$ K, $\Delta C = p = 0$) and hygrothermal vibration ($\Delta T = 60$ K, $\Delta C = 0.02$ %, $p = 0$) of the clamped EGM1 plate resting on elastic foundations are demonstrated in Fig. 8. It is noticed that increments occur for the frequencies as the mode numbers increases. As the side-to-thickness ratio b/h increases, the effects of the mode numbers become more significant.

Fig. 9 illustrates the second frequency Ω_2 of simply supported EGM1 and EGM2 nanoplates for various values the inhomogeneity parameters α and κ, respectively, versus the plate aspect ratio a/b. It is well known the frequencies increase with the increase of rigidity of plate. Since the rigidity of the nanoplates increases by increasing the inhomogeneity parameter α and decreasing the inhomogeneity parameter κ, thus the frequencies increase as α increases and κ decreases.

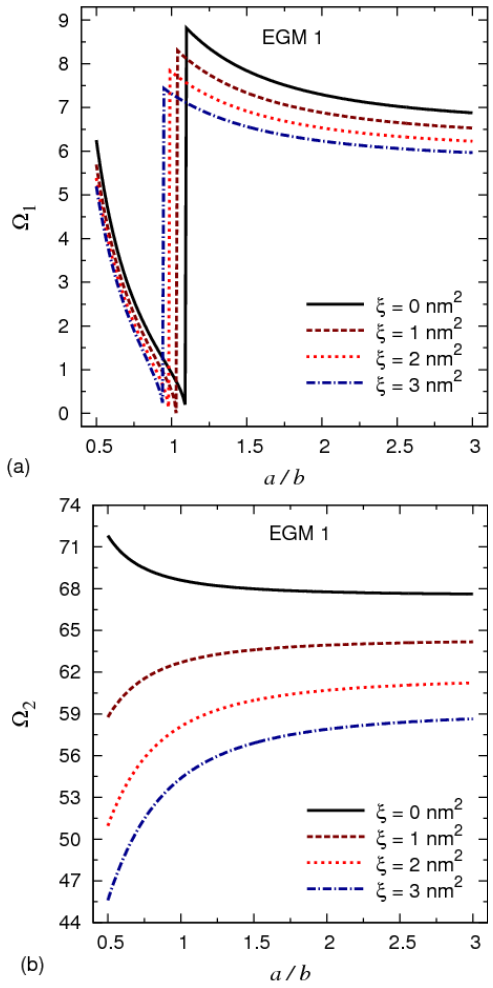

Fig. 5 (a) First dimensionless frequency Ω_1 and (b) second dimensionless frequency Ω_2 of the EGM1 plate versus the plate aspect ratio a/b for various values the nonlocal parameter ξ $(p = 0)$

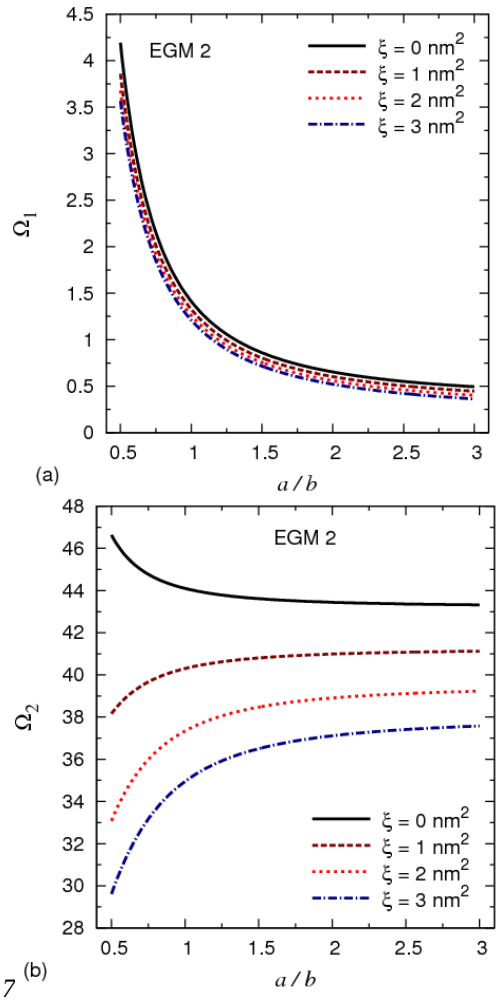

Fig. 6 (a) First dimensionless frequency Ω_1 and (b) second dimensionless frequency Ω_2 of the EGM2 plate versus the plate aspect ratio a/b for various values the nonlocal parameter ξ $(p = 0)$

To investigate how the nonlocal parameter ξ affects the two types of frequencies of the EGM2 nanoplate with different boundary conditions, first and second dimensionless frequencies of EGM2 nanoplate with different eight boundary conditions are plotted in Fig. 10. It is observed that the influences of the boundary conditions on the first frequency Ω_1 are more noticeable when the nonlocal parameter takes smaller values. However, the dependency of the second frequency Ω_2 on the boundary conditions becomes strong when the nonlocal parameter takes greater values. One can also observe from this figure that the FFCC nanoplate undergoes a highest vibration of the first type and a smallest one of the second type. The SSSS nanoplate has the opposite sense.

Fig. 11 displays the effect of the temperature rise and moisture concentration on the buckling load of the EGM2 square plate. It is noted that the increase in the hygrothermal loads reduces the stiffness and strength of the EG nanoplates and then reduces the buckling loads. Irrespective of the variation of temperature and humidity, the buckling load increases to reach its maximum and then decreases as the side-to-thickness ratio b/h increases.

Effects of the elastic foundation parameters and nonlocal parameter ξ on the buckling load Γ of the EGM2 square plate are shown in Fig. 12. It can be seen that the buckling load increases as the foundation stiffnesses increase and the nonlocal parameter decreases.

A decrement occurs for the buckling load as the inhomogeneity parameter α or κ and the aspect ratio a/b increase as shown in Fig. 13.

6. Conclusions

Hygro-thermo-mechanical vibrations and buckling of the EG nanoplates are examined based on various nonlocal four-unknown shear deformation plate theories. The equations of motion and the related boundary conditions are deduced using the principal of virtual work. The motion equations are solved analytically using new functions for the midplane displacements that satisfy the different boundary conditions. The Eringen's nonlocal elasticity theory is employed to consider the small scale effect on the forced frequencies and buckling load. It is found that,

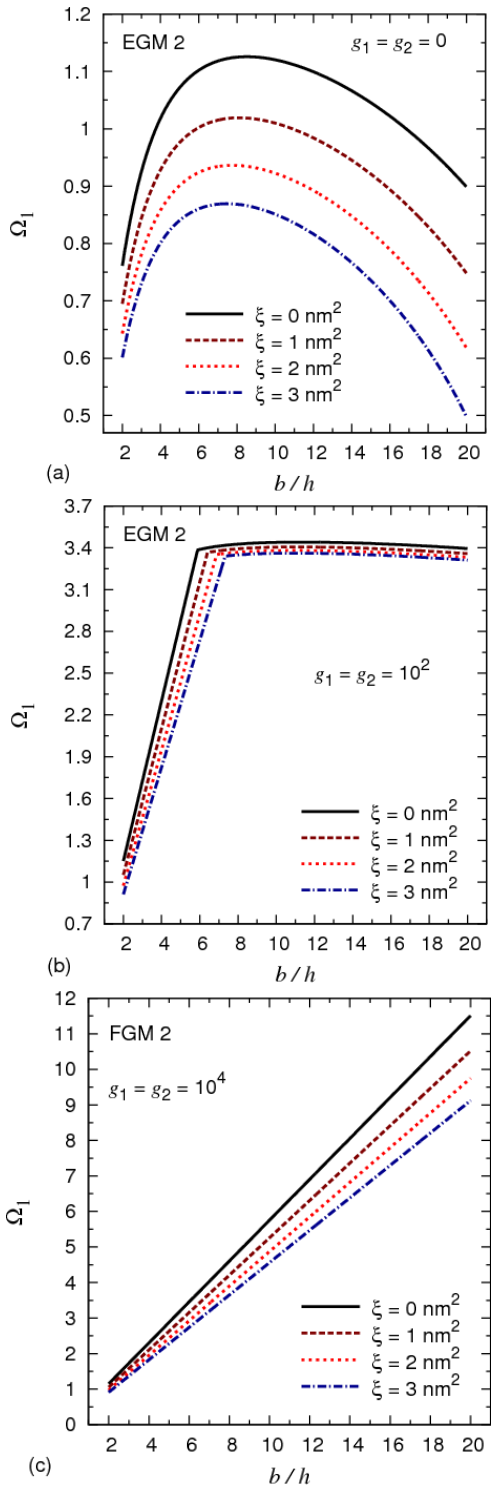

Fig. 7 First dimensionless frequency Ω_1 of the EGM2 square plate versus the side-to-thickness ratio b/h for various values of nonlocal parameter ξ $(p = 0)$ and for (a) $g_1 = g_2 = 0$, (b) $g_1 = g_2 = 10^2$ and (c) $g_1 = g_2 = 10^4$

considering the small scale effect reduces the vibration and buckling of nanoplates thus it cannot be neglected. The rise in the moisture and temperature leads to a decrement in the stiffness and strength of the nanoplates. Therefore, the presence of the temperature, moisture and/or mechanical loads leads to a significant reduction in the frequencies and

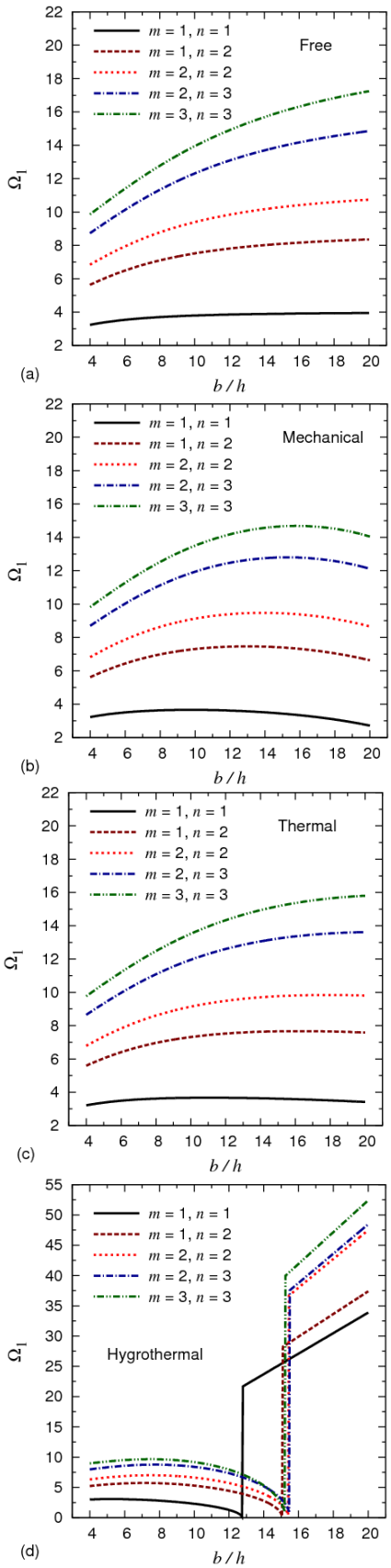

Fig. 8 (a) Free vibration, (b) mechanical vibration, (c) thermal vibration, and (d) hygrothermal vibration of the clamped EGM1 square plate versus the side-to-thickness ratio b/h for various values of the mode numbers m and n $(p = 1$ GPa)

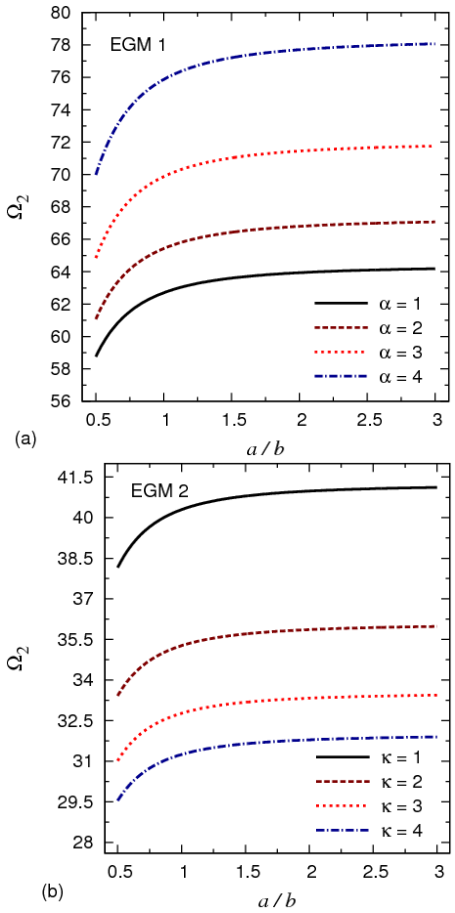

Fig. 9 Second dimensionless frequency Ω_2 of (a) EGM1 plate and (b) EGM2 plate for various values the inhomogeneity parameters α and κ, respectively, versus the plate aspect ratio a/b ($b/h = 10, p = 1\ GPa, \Delta C = 0.1$ %)

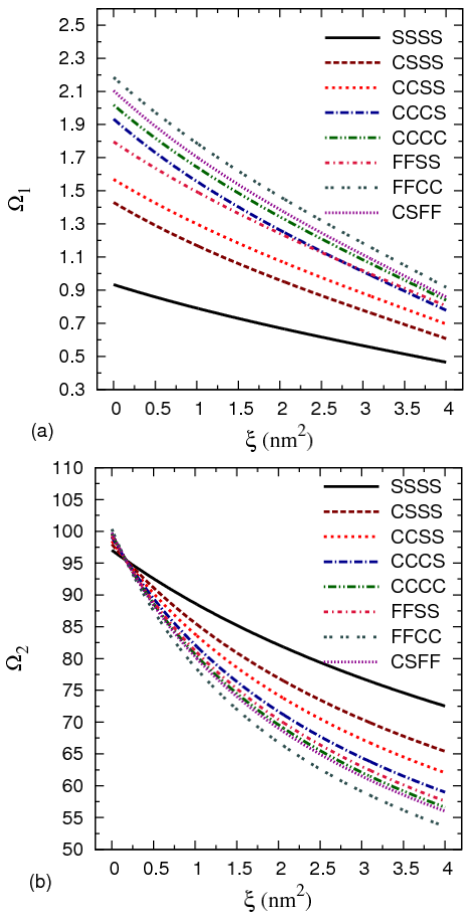

Fig. 10 (a) First dimensionless frequency Ω_1 and (b) second dimensionless frequency Ω_2 of the EGM2 square plate versus the nonlocal parameter ξ for different boundary conditions ($g_1 = g_2 = 100,\ \Delta T = 100\ K,\ p = 10\ GPa$)

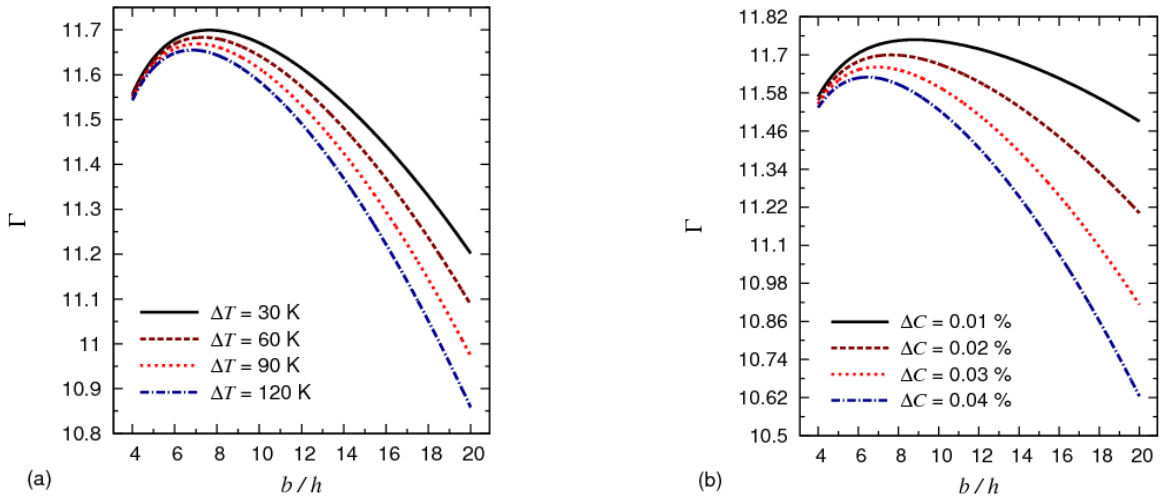

Fig. 11 Buckling load Γ of the EGM2 square plate ($g_1 = g_2 = 100, \xi = 1$ nm^2) versus the side-to-thickness ratio b/h for various values of (a) temperature rise ΔT (ΔC=0.02 %), (b) moisture concentration ΔC (ΔT=30 K)

buckling load. Furthermore, the presence of elastic foundations plays an important role on the vibration and buckling response of the EG nanoplate. The inclusion of the foundation enhances the strength of structures; therefore, the presence of the elastic foundations increases the vibration and buckling load. In addition, the inhomogeneity parameters have great effects on the responses of EG nanoplates. The effects of the plate aspect ratio, side-to-

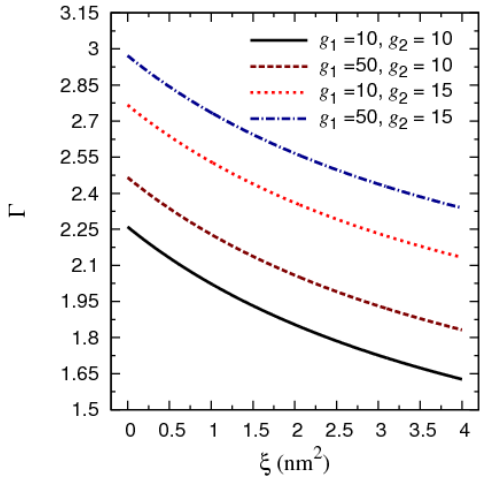

Fig. 12 Effect of the elastic foundation parameters on the buckling load Γ of the EGM2 square plate for various values of the nonlocal parameter ξ (ΔT=100 K, ΔC=0.02 %, $b/h = 10$)

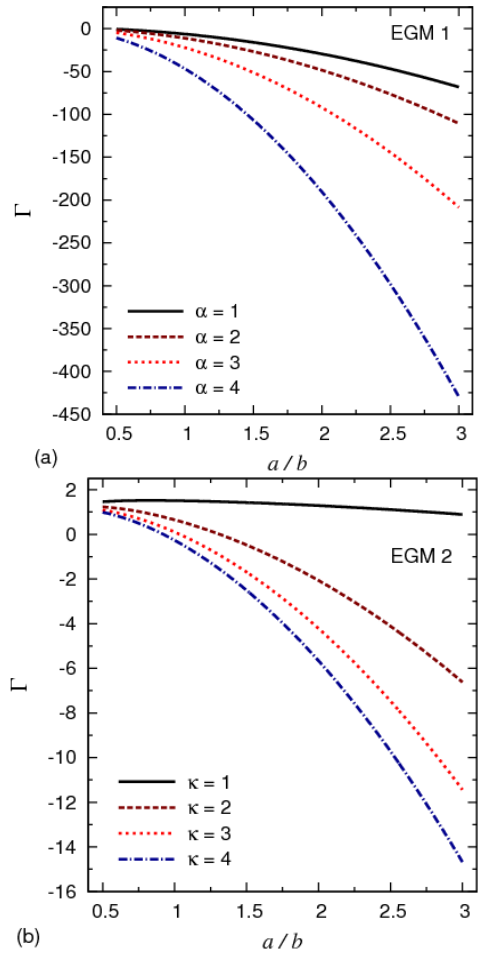

Fig. 13 Buckling load Γ of (a) EGM1 plate and (b) EGM2 plate for various values the inhomogeneity parameters α and κ, respectively, versus the plate aspect ratio a/b ($b/h = 10$, $\Delta C = 0.1$ %)

thickness ratio, boundary conditions and mode numbers on the vibration responses of EG nanoplates are precisely discussed.

Acknowledgements

This project was funded by the Deanship of Scientific Research (DSR), King Faisal University, Hofuf, under grant no. (160028). The author, therefore, acknowledge with thanks DSR technical and financial support.

References

Aghababaei, R. and Reddy, J.N. (2009), "Nonlocal third-order shear deformation plate theory with application to bending and vibration of plates", *J. Sound Vib.* **326**(1), 277-289.

Akavci, S.S. (2014), "Thermal buckling analysis of functionally graded plates on an elastic foundation according to a hyperbolic shear deformation theory", *Mech. Compos. Mater.*, **50**(2), 197-212.

Aydogdu, M. and Taskin, V. (2007), "Free vibration analysis of functionally graded beams with simply supported edges", *Mater. Des.*, **28**, 1651-1656.

Baferani, A.H., Saidi, A.R. and Ehteshami, H. (2011), "Accurate solution for free vibration analysis of functionally graded thick rectangular plates resting on elastic foundation", *Compos. Struct.*, **93**(7), 1842-1853.

Beldjelili, Y., Tounsi, A. and Mahmoud, S.R. (2016), "Hygro-thermo-mechanical bending of S-FGM plates resting on variable elastic foundations using a four-variable trigonometric plate theory", *Smart Struct. Syst.*, **18**(4), 755-786.

Belkorissat, I., Houari, M.S.A., Tounsi, A., Adda Bedia, E.A. and Mahmoud, S.R. (2015), "On vibration properties of functionally graded nano-plate using a new nonlocal refined four variable model", *Steel Compos. Struct.*, **18**(4), 1063-1081.

Bouafia, K., Kaci, A., Houari, M.S.A., Benzair, A. and Tounsi, A. (2017), "A nonlocal quasi-3D theory for bending and free flexural vibration behaviors of functionally graded nanobeams", *Smart Struct. Syst.*, **19**(2), 115-126

Bouderba, B., Houari, M.S.A., Tounsi, A., and Mahmoud, S.R. (2016), "Thermal stability of functionally graded sandwich plates using a simple shear deformation theory", *Struct Eng. Mech.*, **58**(3), 397-422.

Bounouara, F., Benrahou, K.H., Belkorissat, I. and Tounsi, A. (2016), "A nonlocal zeroth-order shear deformation theory for free vibration of functionally graded nanoscale plates resting on elastic foundation", *Steel Compos. Struct.*, **20**(2), 227 - 249.

Cheng, Z.Q. and Batra, R.C. (2000), "Deflection relationships between the homogeneous Kirchhoff plate theory and different functionally graded plate theories", *Arch. Mech.*, **52**, 143-158.

Craciunescu, C.M. and Wuttig, M. (2003), "New ferromagnetic and functionally grade shape memory alloys", *J. Optoelectron. Adv. Mater.*, **5**(1), 139-146.

Eltaher, M.A., Emam, S.A. and Mahmoud, F.F. (2012), "Free vibration analysis of functionally graded size-dependent nanobeams", *Appl. Math. Comput.*, **218**(14), 7406-7420.

Eringen, A.C. (1983), "ON differential-equations of nonlocal elasticity and solutions of screw dislocation and surface-waves", *J. Appl. Phys.* **54**, 4703-4710.

Eringen, A.C. (2002), *Nonlocal Continuum Field Theories*, Springer, New York, USA.

Eringen, A.C. and Edelen, D.G.B. (1972), "On nonlocal elasticity", *Int. J. Eng. Sci.*, **10**, 233-248.

Fu, Y., Du, H. and Zhang, S. (2003), "Functionally graded TiN/TiNi shape memory alloy films", *J. Mater. Lett.*, **57**(20), 2995-2999.

Fu, Y., Du, H., Huang, W., Zhang, S. and Hu, M. (2004), "TiNi-based thin films in MEMS applications: a review", *Sens. Actuat. A - Phys.*, **112**(2-3), 395-408.

Hashemi, S.H., Bedroud, M. and Nazemnezhad, R. (2013), "An exact analytical solution for free vibration of functionally graded circular/annular Mindlin nanoplates via nonlocal elasticity", *Compos. Struct.*, **103**, 108-118.

Janghorban, M. and Zare, A. (2011), "Free vibration analysis of functionally graded carbon nanotubes with variable thickness by differential quadrature method", *Physica E*, **43**, 1602-1604.

Karama, M., Afaq, K.S. and Mistou, S. (2003), "Mechanical behaviour of laminated composite beam by the new multi-layered laminated composite structures model with transverse shear stress continuity", *Int. J. Solids Struct.*, **40**(6), 1525-1546.

Lam, K.Y., Wang, C.M. and He, X.Q. (2000), "Canonical exact solutions for Levy-plates on two-parameter foundation using Green's functions", *Eng. Struct.*, **22**(4), 364-378.

Lee, Z., Ophus, C., Fischer, L.M., Nelson-Fitzpatrick, N., Westra, K.L., Evoy, S. *et al*. (2006), "Metallic NEMS components fabricated from nanocomposite Al-Mo films", *J. Nanotechnol.*, **17**(12), 3063-3070.

Lü, C.F., Lim, C.W. and Chen, W.Q. (2009), "Size-dependent elastic behavior of FGM ultra-thin films based on generalized refined theory", *Int. J. Solid. Struct.*, **46**, 1176-1185.

Merdaci, S., Tounsi, A., Houari, M.S.A., Mechab, I., Hebali, H. and Benyoucef, S. (2011), "Two new refined shear displacement models for functionally graded sandwich plates", *Arch. Appl. Mech.*, **81**(11), 1507-1522.

Meziane, M.A.A., Abdelaziz, H.H. and Tounsi, A. (2014), "An efficient and simple refined theory for buckling and free vibration of exponentially graded sandwich plates under various boundary conditions", *J. Sandw. Struct. Mater.*, **16**(3), 293-318.

Narendar, S. and Gopalakrishnan, S. (2012), "Scale effects on buckling analysis of orthotropic nanoplates based on nonlocal two-variable refined plate theory", *Acta Mech.*, **223**, 395-413.

Natarajan, S., Chakraborty, S., Thangavel, M., Bordas, S. and Rabczuk, T. (2012), "Size-dependent free flexural vibration behavior of functionally graded nanoplates", *Comput. Mater. Sci.*, **65**, 74-80.

Nazemnezhad, R. and Hashemi, S.H. (2014), "Nonlocal nonlinear free vibration of functionally graded nanobeams", *Compos. Struct.*, **110**, 192-199.

Neves, A.M.A., Ferreira, A.J.M., Carrera, E., Cinefra, M., Roque, C.M.C., Jorge, R.M.N. and Soares, C.M.M. (2012), "A quasi-3D hyperbolic shear deformation theory for the static and free vibration analysis of functionally graded plates", *Compos. Struct.*, **94** 1814-1825.

Neves, A.M.A., Ferreira, A.J.M., Carrera, E., Roque, C.M.C., Cinefra, M., Jorge, R.M.N. and Soares, C.M.M. (2011), "Bending of FGM plates by a sinusoidal plate formulation and collocation with radial basis functions", *Mech. Res. Commun.*, **38**, 368-371.

Qian, L.F., Batra, R.C. and Chen, L.M. (2003), "Free and forced vibrations of thick rectangular plates by using higher-order shear and normal deformable plate theory and meshless local Petrov-Galerkin (MLPG)", *Comput. Model. Eng. Sci.*, **4**, 519-534.

Rahaeifard, M., Kahrobaiyan, M.H. and Ahmadian, M.T. (2009), "Sensitivity analysis of atomic force microscope cantilever made of functionally graded materials", *DETC 2009-86254, 3rd international conference on micro- and nano-systems (MNS3)*, San Diego, CA, August-September.

Reddy, J. (1984), "A refined nonlinear theory of plates with transverse shear deformation", *Int. J. Solid. Struct.*, **20**(9), 881-896.

Reddy, J.N. (2000), "Analysis of functionally graded plates", *Int. J. Numer. Meth. Eng.*, **47**, 663-684.

Roque, C.M.C., Ferreira, A.J.M. and Jorge, R.M.N. (2007), "A radial basis function approach for the free vibration analysis of functionally graded plates using a refined theory", *J. Sound Vib.*, **300**, 1048-1070.

Shen, H.S., Chen, Y. and Yang, J. (2003), "Bending and vibration characteristics of a strengthened plate under various boundary conditions", *Eng. Struct.*, **25**(9), 1157-1168.

Shimpi, R.P. (2002), "Refined plate theory and its variants", *AIAA J.*, **40**, 137-46.

Shimpi, R.P. and Patel, H.G. (2006), "Free vibrations of plate using two variable refined plate theory", *J. Sound Vib.*, **296**, 979-999.

Şimşek, M. and Yurtcu, H.H. (2013), "Analytical solutions for bending and buckling of functionally graded nanobeams based on the nonlocal Timoshenko beam theory", *Compos. Struct.*, **97**, 378-86.

Sobhy, M. (2013), "Buckling and free vibration of exponentially graded sandwich plates resting on elastic foundations under various boundary conditions", *Compos. Struct.*, **99**, 76-87.

Sobhy, M. (2014a), "Generalized two-variable plate theory for multi-layered graphene sheets with arbitrary boundary conditions", *Acta Mech.*, **225**, 2521-2538.

Sobhy, M. (2014b), "Natural frequency and buckling of orthotropic nanoplates resting on two-parameter elastic foundations with various boundary conditions", *J. Mech.*, **30**(5), 443-453.

Sobhy, M. (2015a), "Levy-type solution for bending of single-layered graphene sheets in thermal environment using the two-variable plate theory", *Int. J. Mech. Sci.*, **90**, 171-178.

Sobhy, M. (2015b), "A comprehensive study on FGM nanoplates embedded in an elastic medium", *Compos. Struct.*, **134**, 966-980.

Sobhy, M. (2015c), "Hygrothermal deformation of orthotropic nanoplates based on the state-space concept", *Compos. Part B*, **79**, 224-235.

Sobhy, M. (2016a), "Hygrothermal vibration of orthotropic double-layered graphene sheets embedded in an elastic medium using the two-variable plate theory", *Appl. Math. Model.*, **40**, 85-99.

Sobhy, M. (2016b), "An accurate shear deformation theory for vibration and buckling of FGM sandwich plates in hygrothermal environment", *Int. J. Mech. Sci.*, **110**, 62-77.

Sobhy, M., and Radwan, A.F. (2017), "A new quasi 3D nonlocal plate theory for vibration and buckling of FGM nanoplates", *Int. J. Appl. Mech.*, **9**(1), 1750008.

Soldatos, K.P. (1992), "A transverse shear deformation theory for homogeneous monoclinic plates", *Acta Mech.*, **94**, 195-220.

Srinivas, S., Rao, C.V.J. and Rao, A.K. (1970), "An exact analysis for vibration of simply-supported homogeneous and laminated thick rectangular plates", *J. Sound Vib.*, **12**(2), 187-199.

Thai, C.H., Ferreira, A.J.M., Bordas, S.P.A., Rabczuk, T., and Nguyen-Xuan, H. (2014), "Isogeometric analysis of laminated composite and sandwich plates using a new inverse trigonometric shear deformation theory", *Eur. J. Mech.-A/Solid.*, **43**, 89-108.

Thai, C.H., Nguyen-Xuan, H., Bordas, S.P.A., Nguyen-Thanh, N., and Rabczuk, T. (2015), Isogeometric analysis of laminated composite plates using the higher-order shear deformation theory", *Mech. Adv. Mater. Struct.*, **22**(6), 451-469.

Thai, H.T. and Choi, D.H. (2011), "A refined plate theory for functionally graded plates resting on elastic foundation", *Compos. Sci. Technol.*, **71**(16), 1850-1858.

Thai, H.T., Nguyen, T.K., Vo, T.P. and Lee, J. (2014), "Analysis of functionally graded sandwich plates using a new first-order shear deformation theory", *Eur. J. Mech.-A/Solid.*, **45**, 211-225.

Touratier, M. (1991), "An efficient standard plate theory", *Int. J. Eng. Sci.*, **29**(8), 901-916.

Wang, Q. and Wang, C.M. (2007), "The constitutive relation and small scale parameter of nonlocal continuum mechanics for modelling carbon nanotubes", *Nanotechnol.*, **18**(7), 075702.

Witvrouw, A. and Mehta, A. (2005), "The use of functionally graded poly-SiGe layers for MEMS applications", *Mater. Sci. Forum.*, **492-493**, 255-260.

Zemri, A., Houari, M.S.A., Bousahla, A.A. and Tounsi, A. (2015), "A mechanical response of functionally graded nanoscale beam: an assessment of a refined nonlocal shear deformation theory beam theory", *Struct. Eng. Mech.*, **54**(4), 693-710.

Zenkour, A.M. and Sobhy, M. (2010), "Thermal buckling of various types of FGM sandwich plates", *Compos. Struct.*, **93**, 93-102.

Zenkour, A.M. and Sobhy, M. (2011), "Thermal buckling of functionally graded plates resting on elastic foundations using the trigonometric theory", *J. Therm. Stress.*, **34**, 1119-1138.

Zenkour, A.M. and Sobhy, M. (2012), "Elastic foundation analysis of uniformly loaded functionally graded viscoelastic sandwich plates", *J. Mech.*, **28**, 439-452.

Zenkour, A.M. and Sobhy, M. (2013), "Dynamic bending response of thermoelastic functionally graded plates resting on elastic foundations", *Aerosp. Sci. Technol.*, **29**, 7-17.

CC